Defence Science Journal, Vol. 71, No. 3, May 2021, pp. 352-358, DOI : 10.14429/dsj.71.16704

Compact Wideband Microstrip Patch Antenna Design for Breast Cancer Detection

Rakesh Singh[#], Naina Narang[#,@], Dharmendra Singh[#,*], and Manoj Gupta[$]

[#]*Department of Electronics and Communication, Indian Institute of Technology Roorkee, Roorkee - 247 667, India*
[@]*Department of Computer and Communication Engineering, Manipal University Jaipur, Jaipur - 303 007, India*
[$]*Department of Radiation Oncology, All India Institute of Medical Sciences, Rishikesh - 249203, India*
[*]*E-mail: dharm@ec.iitr.ac.in*

ABSTRACT

The current breast cancer detection techniques are mostly invasive and suffer from high cost, high false rate and inefficacy in early detection. These limitations can be subdued by the development of a non-invasive microwave detection system whose performance is predominantly dependent on the antenna used in the system. The designing of a compact wideband antenna and matching its impedance with breast phantom is a challenging task. In this paper, we have designed a compact antenna matched with the breast phantom operating in wideband frequency from 1 to 6 GHz capable to detect the dielectric (or impedance) contrast of the benign and malignant tissue. The impedance of the antenna is matched to a cubically shaped breast phantom and a very small tumor (volume=1 cm^3). The antenna is tuned to the possible range of electrical properties of breast phantom and tumour (permittivity ranging from 10 to 20 and conductivity from 1.5 to 2.5 S/m). The return loss (S_{11}), E-field distribution and specific absorption rate (SAR) are simulated. The operating band of antenna placed near the phantom without the tumor was found to be (1.11-5.47)GHz and with tumor inside the phantom is (1.29-5.50)GHz. Results also show that the SAR of the antenna is within the safety limit.

Keywords: Breast tissue; Microwave; Malignant tissue; Phantom; Radar-based imaging

1. INTRODUCTION

According to world health organisation, every year 2.1 million women are diagnosed with breast cancer worldwide[1]. It is reported that in every four minutes, an Indian woman diagnosed with breast cancer. In every 2 women diagnosed with breast cancer, one women dies in India. Thereby, in every 13 minutes, one women dies of breast cancer in India[2]. Although breast cancer cases in India are lower than western country, India is highly populated so the risk of breast cancer is high. Breast cancer generally develops in the lobules or in the ducts which connects to the nipple and the cells of breast tissue changes uncontrollably. The existing diagnosis and detection techniques have several limitations, such as high cost, high false rate, patients inconvenience, etc., which motivates researchers to find a different approach for the early detection of breast cancer[3]. There has been requirement for a new noninvasive, nonionising, and cost-effective system for breast tumor detection. In breast cancer, dielectric properties of cells vary with respect to the size of the tumor. The electrical properties of breast phantom at the microwave frequency significantly differ with malignant breast tissue. Earlier some studies has been reported on the basis of dielectric contrast between normal and malignant tissue at the microwave frequency[4]. Broadly, two approaches are used in microwave imaging: (1) tomography based and (2) radar based. In microwave tomography, the breast is illuminated by a transmitter and scattered signals are measured. The collected signals coming from breast phantom are used to reconstruct the complex permittivity distribution in the breast phantom[5]. Radar based imaging transmit the signal through an antenna and received the signal through same or another antenna. Antenna is scanned number of location surrounding the breast phantom, and this process is repeated again and again[6].

Several antennas have been proposed and used in radar-based imaging for the detection of the breast tumor. Flexible 16 antenna array antenna has been designed for breast cancer detection[7].Wearable conformal antenna arrays has been used for breast cancer detection[8]. A Q-slot monopole antenna designed for body centric communication[9].ultra wideband near field imaging system has been designed for breast cancer detection[10]. The breast cancer treatment using radar-based approach uses the wideband or ultra-wideband signal. The different shape of antenna has been used for detection of the breast tumor. A wearable flexible antenna has been designed for breast tumor screening[11].A compact body matched antenna bowtie antenna has been designed for medical diagnosis. On body matched antenna provides the more radiated energy into the human body[12]. However, radiation at lower frequency is required for deeper penetration of breast tissue. Radiation near to 1 GHz is favorable for sufficient penetration into the breast tissue. Since the antenna dimension is directly related to the wavelength of the signal, currently it is very difficult to design a compact antenna that covers lower frequency. Also designing of a matched antenna with breast tissue is a challenging task.

Received : 22 January 2021, Revised : 02 February 2021
Accepted : 04 February 2021, Online published : 17 May 2021

In this paper, a detailed design and characterisation process is explained for development of microstrip circular patch antenna that can be used as a sensor for detecting breast cancer. The proposed antenna is developed by properly matching it with the breast phantom having varying electrical properties, i.e. permittivity and conductivity. In the proposed antenna design, the frequency response of S_{11} parameter is tuned with the dielectric properties of breast tissue and also the size of the tumor.

2. THEORETICAL CONSIDERATION

In this section, the basic principles involved in microwave imaging and miniaturisation of antenna required for imaging are discussed in detail.

2.1 Basic Concepts of Microwave Imaging

The basic principle of microwave imaging is to send microwave signals into human tissue and analyse changes in the back-scattered signal, which reflect differences in the electrical properties of tissues. The remarkable variations in the back-scattered signal can be used to identify unwanted tumor cells inside the breast, which exhibit higher dielectric constants than normal breast tissues. The dielectric properties of the breast phantom changes with the insertion of the tumor cell and their effective dielectric constant of phantom with the tumor may be calculated using the well-known Maxwell Garnett equation[13]

$$\varepsilon_{eff} = \varepsilon_m + 3\varepsilon_m \phi_v \frac{(\varepsilon_p - \varepsilon_m)}{2\varepsilon_m + \varepsilon_p - \phi_v(\varepsilon_p - \varepsilon_m)} \quad (1)$$

where ε_m and ε_p are the permittivity of host and inclusion and ϕ_v is the volume fraction of inclusion. Here, the phantom and tumor work as the host material and inclusion, respectively. The altered permittivity of the phantom with the inclusion of the tumor is the key factor leveraged in the microwave imaging system. Thereby, a sensor sensitive enough to identify the variation of permittivity is crucial.

Further, while implementing microwave imaging, another crucial parameter is the penetration depth in the breast phantom which is inversely related to the attenuation coefficient α (Np/m), that is penetration (or skin) depth in phantom,

$$\delta = \frac{1}{\alpha} \quad (2)$$

The attenuation coefficient depends on frequency and dielectric properties of breast phantom and is given in Np/m as

$$\alpha = \omega \sqrt{\frac{\mu\varepsilon}{2}\left(\sqrt{1+\left(\frac{\sigma}{\omega\varepsilon}\right)^2} - 1\right)} \quad (3)$$

Considering that the proposed antenna will be used in the detection of the tumor in the breast phantom, therefore the plane wave will be travelling through a lossy medium of breast phantom and its intrinsic impedance will be given as

$$\eta = \sqrt{\frac{j\omega\mu}{\sigma + j\omega\varepsilon}} \quad (4)$$

This will be considered as the impedance of the medium while matching the proposed antenna with the breast phantom i.e., for ω=4 GHz, σ=1.5 S/m, $\mu = 4\pi\times10^{-7}$, $\varepsilon_r = 10$, the calculated impedance will be $\eta = 108.99\angle 17.143$. While simulating the antenna design, the impedance will thus be matched to this value.

If a suitable matched sensor is developed with the required penetration capability, in the present kind of study, the specific absorption rate (SAR) is a vital safety compliance parameter. Technically, SAR is a measure of the rate at which energy is absorbed by per unit mass by phantom. The specific absorption rate can be calculated using the electric field inside the phantom as

$$SAR = \frac{\sigma E^2}{\rho}(w/kg) \quad (5)$$

where, E is the electric field inside the phantom, σ and ρ are the conductivity and mass density of phantom, respectively[14]. The SAR value of the designed antenna has to be in a permissible range for its possible use in medical applications and thereby shall be computed.

2.2 Compact Antenna used in Microwave Imaging

Further, antenna sensors play a key role in microwave imaging systems. To generate the E-field, a microstrip patch antenna can be readily used due to their small size, light weight and planar structure. In the rectangular patch antenna, the order of the mode can be changed by changing the relative dimension of length and width of the patch. However, in circular patch antenna design, there is only one degree of freedom to control the mode i.e., the radius of the circular patch. The variation of radius does not change the operating mode and resonant frequency of the antenna. The radius of the circular patch a can be calculated by equation (6)[15]

$$a = \frac{F}{\left\{1 + \frac{2h}{\pi\varepsilon_r F}\left[\ln\left(\frac{\pi F}{2h}\right) + 1.7726\right]\right\}^{1/2}} \quad (6)$$

where,

$$F = \frac{8.791\times10^9}{f_r\sqrt{\varepsilon_r}} \quad (7)$$

f_r is the resonance frequency, ε_r is the relative permittivity of the substrate and h is the height. It is to be noted here that the operational bandwidth of antenna must be as large as possible to achieve a high range resolution (RR) required to differentiate very small sized tumors. The range resolution is inversely proportional to the operating bandwidth of the antenna, given as $RR=c/(2xBW)$, i.e., wider the band of antenna, finer will be the range resolution. Therefore, a wideband antenna has been proposed and its configuration is discussed in the next section.

3. PROPOSED ANTENNA

In this section, the design of the compact antenna for early detection of breast cancer is discussed in detail. Firstly, the design of the antenna is simulated on HFSS with parameters calculated using the above-mentioned expressions of the circular patch antenna. After the designing and study of performance parameters, i.e. bandwidth and gain of the antenna, its matching with respect to the phantom is explored

through simulation design. The electrical properties of the breast phantom and tumor considered in our study are extracted from literature and are discussed here in brief.

3.1 Proposed Antenna Configuration and its Performance in Free Space

A compact and wideband microstrip patch antenna is proposed for the breast cancer detection system. The geometry of the proposed circular patch antenna is shown in Figs. 1(a) and (b). The substrate used is RT Duroid (ε_r=2.2) due to its low dielectric property and stable radiation property within the operating band. The substrate dimension is 30×30 mm^2 having a thickness of 3 mm. The proposed antenna is based on a circular shaped radiating element. Thereby, the radius of circle is calculated using f_r =4×10^9 (in Hz), substrate permittivity ε_r=2.2 and thickness h=3mm. Substituting these values in equations (6) and (7), the calculated value of F is 1.487 and radius of the circular patch a=9.19 mm. The CPW feed is applied to antenna to improve the impedance matching. CPW fed couples the electromagnetic energy from the input feed line to the radiating patch through a micro-strip line. The antenna with CPW feed reduces the structure complexity and fulfils. The center cylindrical conductor is connected to the rectangular strip line and the outer cylindrical conductor is connected to the ground plane of the antenna. The circular patch on the substrate works as the main radiator of the antenna. Figure 1(c) shows the simulated result of S_{11} parameter of antenna without the phantom. The operating bandwidth of antenna (S_{11}≤-10dB) is from 3.06-5.43 GHz, which is sufficient to provide fine range resolution (~60 mm) for the imaging system. Figure 1 (d) shows the gain plot of the antenna in the boresight direction. The gain of the antenna is approximately 5 dBi in the complete frequency band of interest, suggesting a good radiation capability which is required to impinge the wave into the phantom.

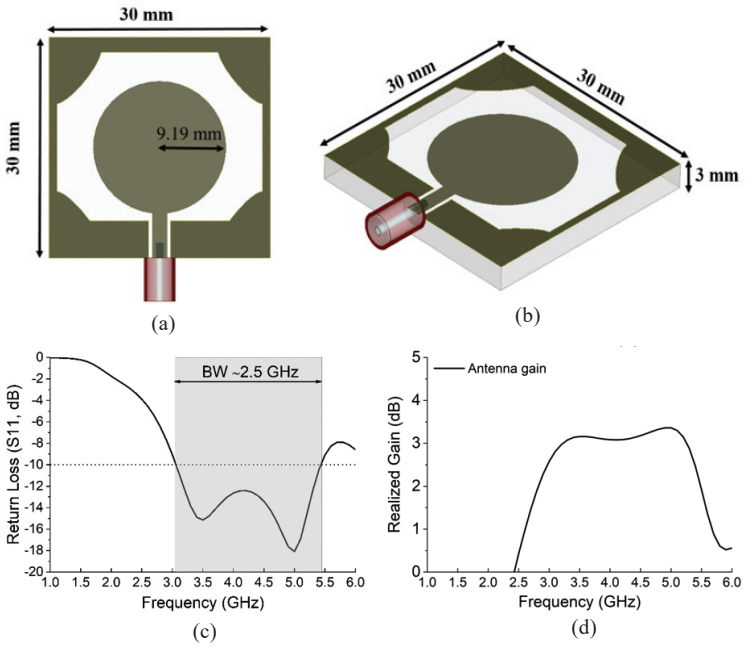

Figure 1. Proposed antenna (a) top view, (b) side view, (c) return loss and (d) realised gain of the antenna.

3.2 Dielectric Properties of Breast Tissue

Designing and development of microwave imaging system requires the knowledge of dielectric properties of human breast tissue. The contrast in the permittivity and conductivity of normal and malignant tissue is the basis for cancer detection using microwave imaging[16]. The difference of dielectric properties occurs due to the varying water percentage in the breast tissue. Water content in fatty tissue is low, thus have a lower relative permittivity and conductivity. Normal tissue consists of high-water content tissues having high relative permittivity and conductivity as compared to fatty tissue at microwave frequency. Further malignant tissue has high water content tissue having high relative permittivity and conductivity as compare to normal and fatty tissue. In this paper, four different type of tissues are considered: fat tissue, normal tissues including the gland tissue and connective tissue, benign tissue and malignant tissue, i.e. breast cancerous tissue. A.M. Campbell and D.V. Land [17] measured the human female breast tissues at 3.2 GHz. The water content in normal breast tissue varies from 41% to 76% by weight and in benign tissue 62% to 84 % by weight and in malignant tissue water content ranged from 66% to 79 % by weight. Human breast cancer tissues have high relative permittivity 45-60, and high conductivity 30-40 mS/cm and 75%-80% water by weight[17]. Conductivity of the breast phantom varies according to the variation of water percentage in the tumorous cell. Water percentage of malignant tissue is larger than normal tissue in the breast phantom. Table 1 shows the relative permittivity, conductivity and water content for fatty tissue, normal tissue, benign tissue and malignant tissue.

3.3 Simulation of Antenna with Breast Phantom

Table 1. Material properties of fatty, normal, benign and malignant tissue at 3.2 GHz[17]

Tissue type	Relative permittivity	Conductivity (mS/cm)	Water content (% by mass)
Fatty tissue	2.8-7.6	0.54-2.9	11-31
Normal tissue	9.8-46	3.7-34	41-76
Benign tissue	15-67	7-49	62-84
Malignant tissue	9-59	2-34	66-79

The proposed antenna is simulated with breast phantom in HFSS, shown in Fig. 2 (a). The cubical-shaped phantom of 50×50×50 mm^3 size is placed on the top of antenna in direct contact with the radiating patch without any air gap. A good contact between antenna and phantom is needed to allow the propagation of a high portion of energy inside the phantom. For this placement of the phantom over antenna, RF excitation using a planar transmission line i.e. CPW feed is suitable. The proposed antenna is optimised with phantom to obtain a minimum reflection between antenna and phantom. The impedance of the antenna is perfectly matched with impedance of breast phantom such that maximum signal is transmitted into the phantom. The permittivity and conductivity of the phantom are taken as 10 and 1.5 S/m, respectively. The impedance of the phantom (i.e. lossy medium) is calculated using equation

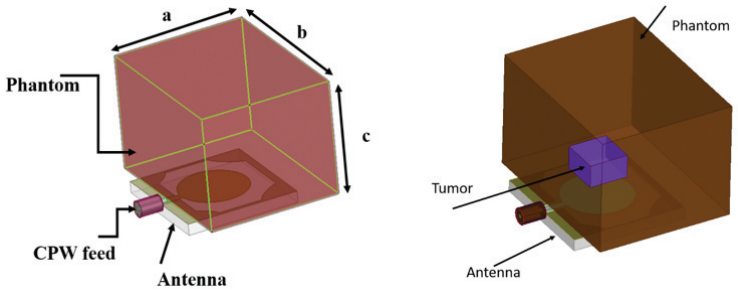

Figure 2. Geometry of proposed antenna with cubical shaped phantom in HFSS (a) without and (b) with tumor.

(4) and found to be $\eta = 108.99\angle 17.143^0$. Further, a cubical-shaped tumor, as shown in Fig. 2 (b), is inserted inside the breast phantom. Initially, the dimension of the cubical shaped tumor is taken as 10×10×10 mm^3 and varied up to 20×20×20 mm^3. The values of permittivity and conductivity of tumor cell are considered as 50 and 3 S/m, respectively. The frequency response of the proposed antenna with the breast phantom has been analysed and given in the next section.

4. RESULTS AND DISCUSSIONS

In this section, the simulated results for the proposed antenna with and without phantom are discussed. The matching of the antenna is dicussed for four scenarios, namely for varied (1) permittivity, (2) conductivity (3) tumor size and (4) analysis with and without the tumor. These variations are important since the human dielectric properties vary from person to person and a matched antenna will be the basic requirement of the imaging system.

4.1 Antenna Performance with and without Phantom

The proposed antenna is designed for microwave imaging application, specifically to detect cancerous cells in the breast. Therefore, the study of wave propagation in the breast phantom is necessary and the effect of the phantom on antenna properties are simulated. The breast phantom is simulated (Fig. 2) considering the dielectric properties of benign and malignant tissues given in Table 1. The radiation performance of the proposed antenna with and without phantom are compared and given in Table 2. Figure 3 shows the radiation pattern of the antenna in the absence and presence of the phantom at three frequencies, 3.5 GHz, 4 GHz and 4.5 GHz. The gain of the antenna drastically decreased if the phantom is in the proximity. The input impedance of the antenna in the absence and presence of the phantom is shown in Fig. 4. It is evident that the capacitive effect of the phantom has caused the decreasing reactance with the increasing frequency.

4.2 Variation of Phantom Permittivity with Fixed Conductivity

Figure 5 shows the simulated S_{11} parameter variation with phantom permittivity. In this simulation, the phantom permittivity 10 and conductivity 1.5 S/m is considered. In this

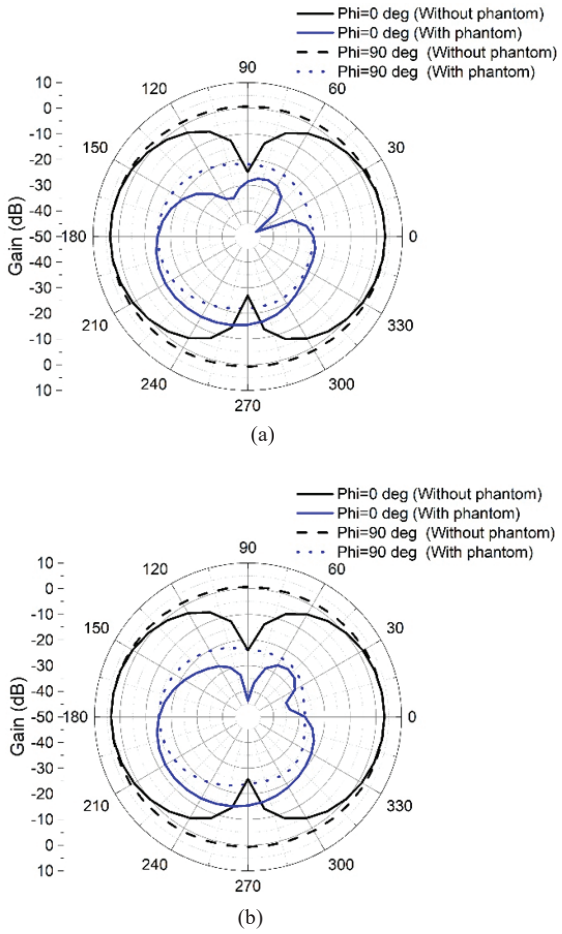

Figure 3. Radiation pattern of the proposed antenna at (a) 3.5 GHz, (b) 4.0 GHz and (c) 4.5 GHz.

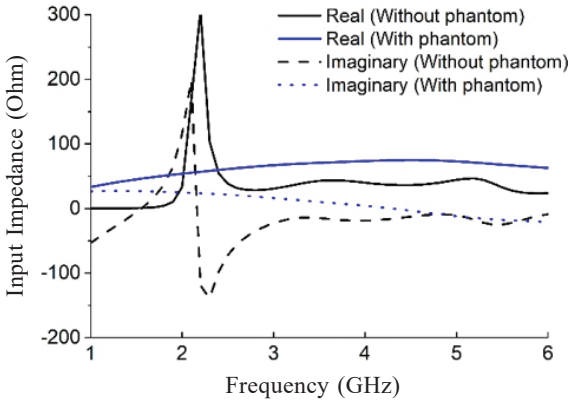

Figure 4. Input impedance of the proposed antenna in free space (without phantom) and with phantom in close proximity.

Table 2. Radiation properties of the proposed antenna with and without the phantom

Freq (GHz)	Peak directivity (dB)		Peak gain (dB)		Peak realised gain (dB)	
	Without phantom	With phantom	Without phantom	With phantom	Without phantom	With phantom
3.5	2.18	4.28	2.20	0.0484	2.133	0.0467
4	2.23	5.32	2.26	0.0551	2.139	0.0530
4.5	2.31	5.61	2.35	0.0557	2.244	0.0534

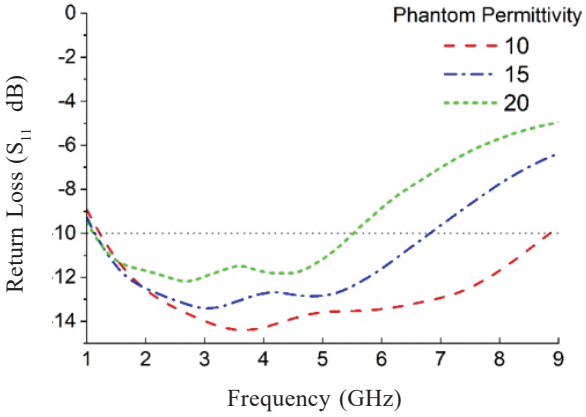

Figure 5. S_{11} parameter variation with different phantom permittivity values.

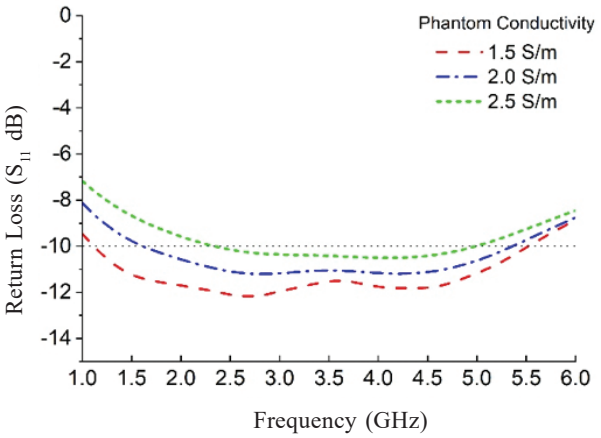

Figure 6. S_{11} parameter of antenna with variation of phantom conductivity.

figure frequency response of S_{11} parameter the lower frequency point cut the -10 dB line at 1.22 GHz and the upper frequency point cut the -10 dB line at 8.86 GHz. Operating band of the antenna with phantom permittivity 10 and conductivity 1.5 S/m is (1.12-8.86) GHz. Dielectric properties of phantom vary with the water percentage in tumorous cell. Effective permittivity and conductivity of phantom changes with the variation of dielectric properties of tumorous tissue. In parametric study phantom permittivity changed from 10 to 15 and phantom conductivity remain fixed 1.5 S/m. The frequency response of the simulated S_{11} parameter cut the -10 dB line at lower frequency point 1.14 GHz and upper frequency point 6.82 GHz. Antenna simulation with phantom permittivity 15 provides the impedance bandwidth of ($S_{11}\leq$-10) within frequency ranges 1.14 GHz to 6.82 GHz. similarly, in next part of simulation phantom permittivity varies from 15 to 20 and conductivity remain fixed throughout the simulation. In this simulation result frequency response of S_{11} parameter the lower frequency point cut the -10 dB line at 1.12 GHz and the upper frequency point cut the -10 dB line at 5.51 GHz. Antenna with phantom permittivity 20 provides the impedance bandwidth of ($S_{11}\leq$ -10 dB) within frequency ranges 1.12 GHz to 5.51 GHz. The operating band of proposed antenna with the phantom shifted left side with variation of phantom permittivity. The antenna resonant frequency point is tuned with phantom permittivity. As the phantom permittivity varied from 10 to 15 and 15 to 20 upper frequency point shifted from 8.86 GHz to 6.82 GHz and 6.82 GHz to 5.51 GHz.

4.3 Variation of Phantom Conductivity with Fixed Permittivity

Figure 6 shows the simulated frequency response of S_{11} parameter of the proposed antenna with variation of phantom conductivity. In this simulation antenna is simulated with cubical shaped phantom placed on the top of the antenna. Antenna simulated with phantom conductivity varied from 1.5 S/m to 2 S/m and 2 S/m to 2.5 S/m and phantom permittivity 20 remain fixed throughout the simulation. Antenna with phantom conductivity 1.5 S/m provides the ($S_{11}\leq$-10) within the frequency range 1.12 GHz to 5.51 GHz. Further antenna simulated with phantom conductivity 2.0 S/m. Antenna with phantom conductivity 2 S/m provides the ($S_{11}\leq$-10) within the frequency range 1.62 GHz to 5.36 GHz. Again, antenna simulated with phantom conductivity 2.5 S/m. antenna with phantom permittivity 2.5 S/m provides the impedance bandwidth from 2.34 GHz to 5.0 GHz. The simulation result shows the operating band of antenna reduces with variation of phantom conductivity. As the phantom permittivity varied from 1.5 S/m to 2 S/m operating band of antenna shifted from 1.12-5.51 GHz to 1.62 -5.36 GHz and with variation of phantom conductivity from 2 S/m to 2.5 S/m operating band of antenna shifted from 1.62 -5.36 GHz to 2.34 -4.99 GHz.

4.4 Variation of Tumor Size

A cubical shaped tumor is inserted inside the phantom. Antenna is simulated with phantom and inserted a cubical-shaped tumor. The tumor has dielectric permittivity and conductivity are 50 and 3 S/m, respectively. Figure 7 shows the variation of S_{11} parameter with tumor size. In this simulation, the tumor size is varied from 10×10×10 mm^3 to 20×20×20mm^3. The operating band of antenna with tumor size 10×10×10 mm^3 is from 1.65 GHz to 5.26 GHz, with tumor size 15×15×15 mm^3 is (1.74 -5.19) GHz and with tumor size 20×20×20 mm^3 is from (1.97- 5.19) GHz.

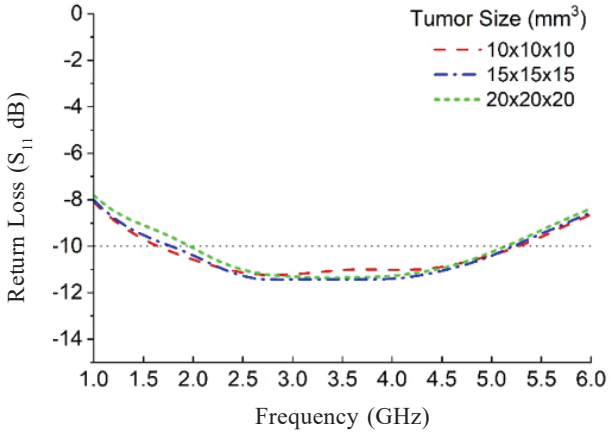

Figure 7. S_{11} variation with tumor size.

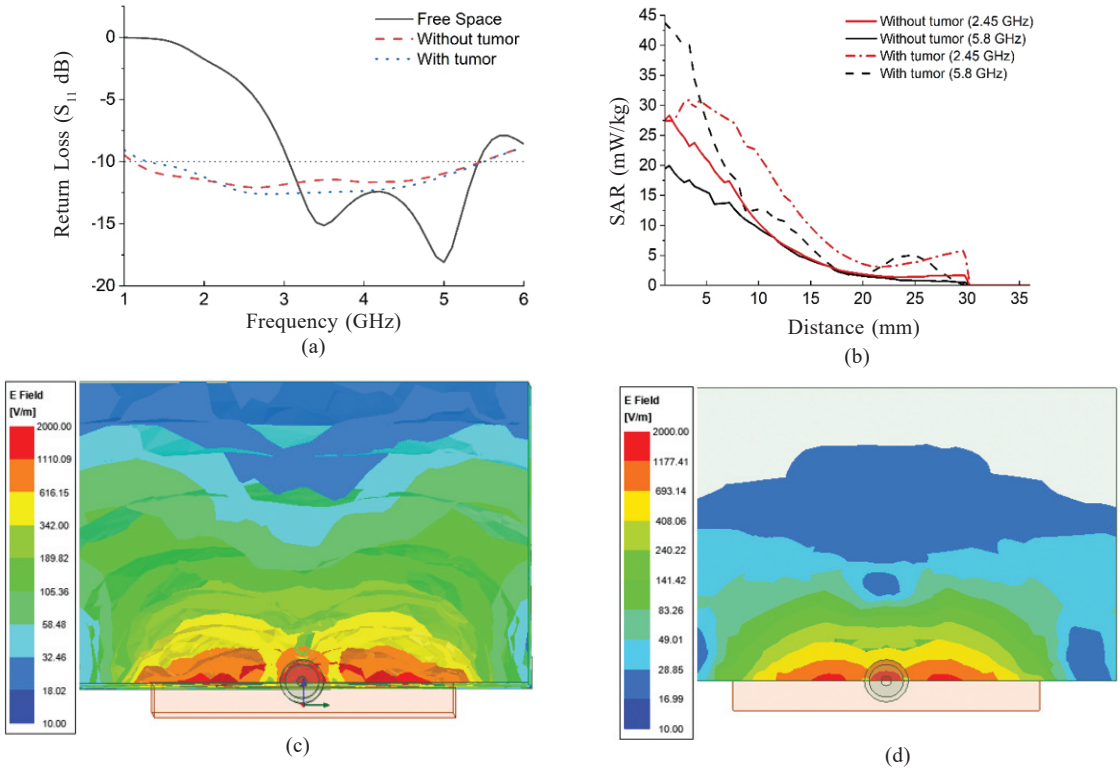

Figure 8. Effect of tumor in the phantom (a) return loss, (b) SAR versus distance between the antenna and point of observation, and E-field strength (c) without and (d) with tumor.

4.5 Analysis With and Without Tumor

Lastly, the antenna is studied with and without the tumor in the phantom. The cubical-shaped tumor of 10×10×10 mm^3 size is considered in the phantom and simulated with antenna. The phantom permittivity and conductivity are 20 and 1.5 S/m, respectively. The dielectric properties of tumor permittivity and conductivity are 50 and 3 S/m. The operating band of antenna without tumor is (1.11-5.47) GHz and the operating band of antenna with tumor inside the breast phantom is (1.29 -5.50) GHz. It is evident from the simulated results (Fig. 8(a)) that the S_{11} parameter with and without the tumor differs very slightly. Figure 8(b) shows the SAR generated by the antenna for two frequencies of interest i.e. 2.45 GHz and 5.8 GHz at various depths inside the phantom along with the E-field distribution inside the two phantoms (Figs. 8(c-d)). As recommended in IEEE standard C95.3[18], the SAR value is within the 2 W/kg limit throughout the complete distance in the phantom. It may be noticed here that the E-field distribution varies significantly and can be the reason for altered SAR values for the two phantoms. Thereby, the proposed antenna can be used as a microwave sensor for biomedical imaging application.

5. CONCLUSIONS

A compact wideband with CPW feed antenna has been designed and simulated with the cubical-shaped phantom and cubical the shaped tumor cell inside the phantom. In simulation four different type of scenarios has been considered. In the first part of simulation, the antenna is characterised for different permittivity of the phantom at a fixed phantom conductivity of 1.5 S/m. As the phantom permittivity was increased, the operating bandwidth of the antenna got reduced at upper frequency. In second part of simulation, the phantom conductivity was varied and phantom permittivity was kept constant at 20. As the phantom conductivity was increased, the operating bandwidth of the antenna was reduced from the lower frequency. In third part of simulation, the size of cubical shaped tumor was varied and a slight change in the bandwidth was observed. Finally, the antenna was simulated with and without tumor. The operating band of antenna without tumor was (1.11-5.47) GHz and the operating band of antenna with inserted tumor inside the breast phantom came out to be (1.29-5.50) GHz. A minor reduction in the operating bandwidth was also found with the increased tumor size. It is concluded that the permittivity of the phantom is most crucial in designing the sensor and the performance of the antenna is independent of the tumor permittivity, conductivity or size. The simulated results have shown good matching of the proposed sensor with the breast phantom and can be vital for the microwave imaging system.

REFERENCES

1. WHO | Breast cancer. https://www.who.int/cancer/prevention/diagnosis-screening/breast-cancer/en/ (Accessed on 14 September 2020).
2. Alarming facts about breast cancer in India | OncoStem Blog. https://www.oncostem.com/blog/alarming-facts-about-breast-cancer-in-india/ (Accessed on 14 September 2020).
3. Fear, E. C.; Hagness, S. C.; Meaney, P. M.; Okoniewski, M. & Stuchly, M. A. Enhancing breast tumor detection with near field imaging. *IEEE Microw. Mag*, 2002, **3**(1), 48–56.

doi:10.1109/6668.990683
4. Loughlin, D. O'; Halloran, M. O'; Moloney, B. M.; Glavin, M.; Jones, E. & Elahi, M. A. Microwave breast imaging: Clinical advances and remaining challenges. *IEEE Trans. Biomed. Eng.*, 2018, **65**(11), 2580–2590. doi: 10.1109/TBME.2018.2809541.
5. Misilmani, H. M. E.; Naous, T.; Khatib, S. K. A. & Kabalan, K. Y. A survey on antenna designs for breast cancer detection using microwave imaging. *IEEE Access*, 2020, **8**, 102570–102594. doi: 10.1109/ACCESS.2020.2999053.
6. Wang, L. Microwave sensors for breast cancer detection. *Sensors (Switzerland)*, 2018, **18**(2), 1–17. doi: 10.3390/s18020655.
7. Bahramiabarghouei, H.; Porter, E.; Santorelli, A.; Gosselin, B.; Popvic, M. & Rusch, A.L. Flexible 16 antenna array for microwave breast cancer detection. *IEEE Trans. Biomed. Eng.* 2015, **62**(10), 2516–2525. doi: 10.1109/TBME.2015.2434956
8. Wang, F.; Arslan, T. & Wang, G. Breast cancer detection with microwave imaging system using wearable conformal antenna arrays. *In* IST 2017 - IEEE International Conference on Imaging Systems and Techniques, 2018, 2018-Jan, 1–6. doi: 10.1109/IST.2017.8261547
9. Yeboah-Akowuah, B.; Kosmas, P. & Chen, Y. A Q-Slot monopole for UWB body-centric wireless communications. *IEEE Trans. Antennas Propag.*, 2017, **65**(10), 5069–5075. doi: 10.1109/TAP.2017.2740977
10. Zwick, T. ; Zwirello, L.; Jalilvand, M. & Li, X. Ultra wideband compact near-field imaging system for breast cancer detection. *IET Microwaves, Antennas Propag.*, 2015, **9**(10), 1009–1014. doi: 10.1049/iet-map.2014.0735
11. Porter, E.; Bahrami, H.; Sabtorelli, A.; Gosselin, B.; Rusch, A.L. & Popovic, M. A wearable microwave antenna array for time-domain breast tumor screening. *IEEE Trans. Medical Imaging,* 2016, **35**(6), 1501–1509. doi: 10.1109/TMI.2016.2518489
12. Li, X.; Jalilvand, M.; Sit, Y. L. & Zwick, T.A compact double-layer on-body matched bowtie antenna for medical diagnosis. *IEEE Trans. Antennas Propag.*, 2014, **62**(4), 1808–1816. doi: 10.1109/TAP.2013.2297158
13. Mishra, V.; Puthucheri, S. & Singh, D. An efficient use of mixing model for computing the effective dielectric and thermal properties of the human head. *Med. Biol. Eng. Comput.*, 2018, **56**(11) 1987–2001. doi: 10.1007/s11517-018-1828-x
14. Narang, N.; Dubey, S.K.; Negi, P.S. & Ojha, V.N. Evaluation of electrical properties of tissue simulating liquids (1.80GHz-2.45GHz) for creating pathways for cancer therapy. *In*11th Int. Conf. Ind. Inf. Syst. ICIIS 2016 - Conf. Proc., 2016, 2018-Jan, pp. 189–192. doi: 10.1109/ICIINFS.2016.8262932
15. Balanis. C.A, Antenna Theory Analysis and Design. *Wiley*. 2005.
16. Martellosio, A.; Pasian, M.; Bozzi, M.; Perregrini, L.; Mazzanti, A.; Svelto, F.; Summers, E.P.; Renne, G.; Preda, L. & Bellomi, M. Dielectric properties characterization from 0.5 to 50 GHz of breast cancer tissues. *IEEE Trans. Microw. Theory Tech.*, 2017, **65**(3), 998–1011. doi: 10.1109/TMTT.2016.2631162.
17. Campbell, A. M. & Land, D. V. Dielectric properties of female human breast tissue measured in vitro at 3.2 GHz. *Phys. Med. Biol.*, 1992, **37**(1), 193–210. doi: 10.1088/0031-9155/37/1/014
18. Institute of Electrical and Electronics Engineers. IEEE recommended practice for measurements and computations of radio frequency electromagnetic fields with respect to human exposure to such fields, 100 kHz to 300 GHz. IEEE C95.3-2002, 2002.

CONTRIBUTORS

Mr Rakesh Singh is pursuing PhD at Department of ECE, IIT Roorkee, India. His research interests include microwave and millimetre wave, antennas for microwave imaging for breast cancer detection.
In this study, he has carried out the simulation work for antenna designing, theoretical concept building and analysis of artificial phantom with antenna and manuscript writing.

Dr Naina Narang, completed her PhD in 2017 from CSIR National Physical Laboratory, New Delhi and thereafter worked as Assistant Professor at Department of Computer and Communication Engineering, Manipal University Jaipur, India for one year and nine months. Presently, she is carrying out her post-doctoral research work in Department of ECE at IIT Roorkee. Her research area includes automated instrument control, simulation techniques and computational electromagnetics.
In this work, she has proposed the methodology and drafted the manuscript.

Dr Dharmendra Singh received the Ph.D. degree in Electronics Engineering from IIT (BHU) Varanasi, Varanasi, India. He has 25 years of experience in teaching and research. He is currently a Professor with the Department of Electronics and Communication Engineering, IIT Roorkee, Roorkee, India, and a Coordinator at RailTel-IIT Roorkee Centre of Excellence in Telecom, Roorkee. His research interests include microwave remote sensing, polarimetry, interferometry, and numerical modelling, through-wall imaging, and stealth technology.
In this study, the problem is defined by him and research work has been carried out under his guidance.

Dr Manoj Gupta is currently working as a professor of radiotherapy at All India of Medical Sciences Rishikesh India. His research interests include neck cancer and breast cancer. In this study, he has looked after the methodology, requirements and efficacy of the proposed design.